Journal of Applied Pharmaceutical Science Vol. 15(07), pp 179-192, July, 2025
Available online at http://www.japsonline.com
DOI: 10.7324/JAPS.2025.221818
ISSN 2231-3354

Bioactivity evaluation of compounds produced by *Fusarium equiseti* from *Kaempferia parviflora* rhizome from Indonesia

Praptiwi Praptiwi[1*], Muhammad Ilyas[2], Agus Budiawan Naro Putra[1], Kartika Dyah Palupi[1], Ahmad Fathoni[1], Puspa D. N. Lotulung[1], Evana Evana[1], Dwinna Rahmi[1], Andria Agusta[1]

[1]Research Center for Pharmaceutical Ingredient and Traditional Medicine, National Research and Innovation Agency (BRIN), Bogor, Indonesia.
[2]Research Center for Biosystematics and Evolution, National Research and Innovation Agency (BRIN), Bogor, Indonesia.

ARTICLE HISTORY

Received on: 05/01/2025
Accepted on: 03/04/2025
Available Online: 05/06/2025

Key words:
Endophytic fungi, *Fusarium equiseti* BwKpRt-1, *Kaempferia parviflora*, bioactivities, LC-HRMS.

ABSTRACT

Endophytic fungi have garnered attention for their ability to synthesize chemical compounds similar to those of their host plants. This study evaluated the bioactivities of BwKpRt-1, an endophytic fungus associated with *Kaempferia parviflora* rhizome. Bioactivity analyses included antioxidant assays, antibacterial, and antiproliferative toward cell lines, identified a fungal species and its chemical compounds using liquid chromatography high resolution mass spectrometry (LC-HRMS). Docking study for equisetin was also carried out in this research. The extract of BwKpRt-1 demonstrated antioxidant activity with an IC_{50} value of 57.36 µg/ml (DPPH) or AAI value of 0.5 (moderate). Its α-amylase and α-glucosidase inhibitory activities were 0.121 ± 0.02 nmole/minute/ml and 335.38 unit/l, respectively. Antibacterial activity is strong against *Staphylococcus aureus* with a minimum inhibitory concentration value of 64 µg/ml. The anticancer activity of this extract against MCF-7 and A549 showed $IC_{50,}$ which were 58.61 and 42.64 µg/ml. Chemical compound analysis using LC-HRMS identified equisetin as a main compound (42.18%). Docking study showed that Equisetin (EQ) exhibits stronger antioxidant and anticancer potential than standard drugs, showing lower energy affinities than vitamin C (VitC) for *Hs*KEAP1 (−8.5 *vs.* −6.1 kcal/mol) and doxorubicin (DXR) for *Hs*EGFR (−8.5 *vs.* −7.8 kcal/mol). Phylogenetic analysis revealed that BwKpRt-1 had a 99.08% similarity to *Fusarium equiseti*. These findings highlight the potential of *F. equiseti* BwKpRt-1 as a source of bioactive compounds for pharmaceutical applications.

INTRODUCTION

One species of the Zingiberaceae that recently gained attention for research is *Kaempferia*. Several plant species from the Zingiberaceae family have been known to have health benefits. *Kaempferia parviflora* has several local names*, i.e.,* Black ginger, Thai ginger, Kalahood (India, Bangladesh), Ingwer (German), Gamin-ni (Burmese), Cekur hitam (Malaysia), Kencur hitam (Indonesia) and Krachai dam (Thailand) [1]. It is native to Thailand, Bangladesh, Cambodia, and Myanmar [2].

According to the plant of the world online, the rhizomes of *K. parviflora* are characterized by their small size and deep purple color. The leaves measure between 8 and 16 cm in length, are thin, green, and have a rounded base. The petioles have narrow canals. Stemless, several flowers are located in a central. The green, lanceolate bracts are around 2.5 cm in length. The tube of corolla is 3 cm long with greenish segments that are 1 cm long, and the calyx reaches beyond the bract, ascending and somewhat concave. The lip measures between 0.75 and 1.0 cm, is sub-marginate, and features an obtuse anther-crest, matching its width to its length.

The rhizome of *K. parviflora* contains several active chemical compounds, *i.e*., saponin, alkaloid, tannin, glycoside, polyphenol, flavonoid, lipophenol, terpene, phenol, and steroid [3]. *K. parviflora* possesses several bioactivities, such as aphrodisiac [4], antiinflammation [5], antiallergic [6], anticancer [7], antiobesity [8], α-glucosidase inhibitory effects [9] and others. These pharmacological effects must be related to the chemical compounds in *K. parviflora.* Due to its antimicrobial properties,

*Corresponding Author
Praptiwi Praptiwi, Research Center for Pharmaceutical Ingredient and Traditional Medicine, National Research and Innovation Agency (BRIN), Bogor, Indonesia. E-mail: praptiwip @ yahoo.com

K. parviflora may be utilized as a natural food additive in various dairy products [10]. There is a high demand for *K. parviflora* rhizome; however, planting is still rare [11]. These conditions are similar to those in Indonesia, so the availability is limited, and the price of *K. parviflora* rhizome is relatively high. Therefore, large-scale exploitation will be another issue, endophyte-based bioactive production has been developed to date.

On the other hand, inside healthy plant tissue was inhabited by endophytic microbes that could classified as fungal endophytes or bacterial endophytes. Endophytes have the capability to produce secondary metabolites that resemble those of their host plant and possess bioactivities [12,13]. Therefore, there is a high possibility of getting host-specific metabolites that have beneficial applications in many sectors, including pharmacy [12]. Endophytes can produce pharmacologically active compounds with antibacterial, antitumor, anticancer, antifungal [12], antiparasitic, and antioxidant activities [13]. Several pure compounds isolated from endophytic fungi have been evaluated for their bioactivity. Equisetin isolated from the fungal endophyte *Chaetomium globosum* could inhibit the growth of several bacteria resistant to multiple drugs [14]. Fungal endophytes isolated from *Azadirachta indica* possess antiplasmidial activity [15]. Comparing secondary metabolite extraction from plants is laborious, time-consuming, and costly [13]; the extraction from endophytic fungi takes a shorter time, is cheaper, and is non-laborious.

Fusarium equiseti is a fungal species and plant pathogen that affects a wide range of crops [16]. It is generally considered a pathogen on wheat and sometimes commonly referred to as *Fusarium* head blight, as one of the most relevant fungal diseases of wheat associated with different fungal species from the genus *Fusarium* [16]. This species is commonly found in tropical and subtropical regions. In 2016, *F. equiseti* was identified as a cause of wilt in *Capsicum chinense* in Mexico. Additionally, it has been reported as one of the fungi responsible for causing chili wilt in Kashmir, alongside other species such as *Fusarium oxysporum* and *Fusarium solani* [17].

In a previous study, an entomogenous fungus of *F. equiseti* LGWB-9, isolated from *Harmonia axyridis*, produced four polyketide derivatives named fusaketide A-B and pestalotiollides A-B. Fusaketide A and B demonstrated potent activity against the MCF-7, MGC-803, HeLa, and Huh-7 cell lines [18]. A marine fungus of *F. equiseti* UBOCC-A-117302 produced six fusarochromanone derivatives along with two other compounds, (−)-chrysogine and equisetin. The six fusarochromanone derivatives exhibited a range of activities against three cell lines (RPE-1, HCT-116, and U2OS). Additionally, equisetin demonstrated bactericidal activity against *Bacillus cereus* and *Listeria monocytogenes* [19].

Based on the research described above, endophytic fungi associated with the plant *K. parviflora*, including *F. equiseti* BwKpRt-1, have not yet been studied for their antibacterial activity against *S. aureus*, antioxidant properties (using DPPH radical scavenging, ABTS, and Ferric reducing antioxidant power (FRAP) methods), antidiabetic potential (as an alpha-glucosidase inhibitor), or anticancer activity (against MCF-7 and A549 cell lines). So, this research aimed to study the endophytic fungi associated with the medicinal plant *K. parviflora*, including the selected endophytic fungus *Fusarium equiseti* BwKpRt-1 extract, to evaluate its bioactivity. The bioactivity was assessed for antibacterial activity against *S. aureus*, antioxidant properties (using DPPH radical free scavenging, ABTS, and FRAP methods), antidiabetic potential (as an alpha-glucosidase inhibitor), and anticancer activity (against MCF-7 and A549 cell lines, and species verification of *F. equiseti* BwKpRt1 using phylogenetic analyses by amplifying rDNA and the chemical compound contained in the ethyl acetate extract of fungal endophyte BwKpRt-1.

MATERIALS AND METHODS

Solvents

Solvents for thin-layer chromatography (TLC) (methanol and dichloromethane) and extraction (ethyl acetate) were technical solvents and were distilled once with a purity of 96%–97%. The solvents used for LC-MS analysis possess a purity of > 99.9 %, which are methanol, water, and acetonitrile, with a purity of 99.8 %, provided by Merck (Germany). Thermo Scientific (USA) supplied the ESI calibration solution for both positive and negative modes.

Plant material

Kaempferia parviflora plants were collected from Bogor and Banyuwangi, Indonesia. The plants were identified in Herbarium Bogoriense, National Research and Innovation Agency (BRIN), Cibinong, Bogor, Indonesia.

Endophytic fungi isolation

Parts of the plants were washed and cut to approximately 1–4 cm, followed by surface sterilization according to Praptiwi *et al*. [20] as follows: soaking in 70% alcohol for 1 minute, followed by soaking in 5.25% NaOCl for 2.5–3.5 minutes, and then dipped again in 70% alcohol for 30 seconds. Sterile samples were dried aseptically, cut into small pieces with sterile blades, placed on the surface of Corn Meal Malt Agar medium supplementing with 0.05 mg/ml chloramphenicol, and incubated for 3–5 days at room temperature. Each fungal colony that was subsequently grown was transferred to a potato dextrose agar (PDA) medium until a single isolate was obtained. The isolates of endophytic fungi No. 1–17 were isolated from *K. parviflora* (from Bogor), and No. 18–20 were isolated from *K. parviflora* (from Banyuwangi). Thus, twenty endophytic fungi from *K. parviflora* were identified in the Indonesian Culture Collection (InaCC), BRIN, Cibinong, Bogor. Pure isolates were preserved in 10% glycerol and stored at –80°C until used.

Cultivation of fungal endophyte BwKpRt1 and extraction of bioactive compounds

Endophytic fungi were scaled up to generate secondary metabolites. The culture of a pure isolate of fungal endophyte BwKpRt1 was re-cultured in 2 L potato dextrose broth (PDB). Two pieces (0.5 × 0.5 cm^2) of endophytic fungus of BwKpRt1 were taken from PDA culture media and placed in a 500 ml culture flask with 200 ml of PDB aseptically. PDB media is commonly employed for screening and scaling up endophytic fungi, as it provides complete nutrition, including carbon

sources (dextrose) and nitrogen (potato). Incubation is carried out under conditions based on previous research, specifically in dark room, at room temperature (25°C), and under static conditions. These conditions are optimal for fungal growth and the production of active compounds, which are less likely to be damaged by light and temperature. Static conditions are also more cost-effective as they do not require a shaker. After that, the culture flasks were kept under dark circumstances at ambient temperature for 3 weeks.

Following incubation, the media and biomass of fungi were soaked using ethyl acetate three times. Based on previous research, semipolar and active compounds are extracted using the liquid-liquid extraction method, where ethyl acetate is used. It forms two layers, distinguishing the liquid medium from the extracted biomass. This method does not require a freeze dryer for the liquid medium and biomass, making it time-saving, relatively simple, and cost-effective. Every maceration takes about 24 hours. The extract was mixed. Then, using an evaporator, the extract was concentrated and kept for future use at 4°C.

Endophytic fungi identification based on morphological characters and molecular identification

A pure fungal isolate was placed on Petri dishes filled with PDA, followed by 7–10 days of incubation. The initial identification of all fungi was conducted based on their morphological characteristics. Both macroscopic and microscopic features were observed for morphological identification from colonies grown on PDA, following the methodology described in our previous study [20].

Selected fungi, such as strain BwKpRT-1, were further identified using molecular techniques. Analyzing the DNA sequence of the internal transcribed spacer (ITS1 and ITS2) regions of rDNA, including the 5.8S rRNA, was necessary for molecular identification. The Nucleon PhytoPure plant and fungal DNA extraction kits were used to isolate the DNA of fungi based on GE Healthcare instructions. Polymerase chain reaction (PCR) was used to amplify the region of ITS rDNA. The molecular identification conducted by analyzing the DNA sequence of an internal transcribed spacer (ITS1 and ITS2) of rDNA regions, includes the 5.8S rRNA. The total fungal genomic DNA was isolated using Nucleon PhytoPure plant and fungal DNA extraction kits (GE Healthcare) according to the manufacturer`s instructions. DNA amplification of the ITS rDNA region was performed by PCR. PCR amplification was performed in 25 µl reaction mixtures containing 10 µl distilled water, 12.5 µl GoTaq Green Master Mix (Promega), 0.5 µl dimethyl sulfoxide (DMSO), 0.5 µl each primer (10 pmol), and 1 µl (5–10 ng) extracted genomic DNA as a template. The primer set of ITS4 (5`-TCCTCCGCTTATTGATATGC-3`) and ITS5 (5`-GGAAGTAAAAGTCGTAACAAGG-3`) was used to amplify approximately 500 nucleotides from ITS1 and ITS 2, including 5.8S rDNA. Amplification was performed in a TaKaRa PCR Thermal Cycler P650 (TAKARA BIO Inc.), programmed under the following conditions: initial denaturation at 95°C for 3 minutes, 30 cycles at 95°C for 30 seconds, 55°C for 30 seconds, and 72°C for 1 minutes. The PCR products were then subjected to purification and sequence analysis.

ChromasPro was used to edit the data of the raw sequence of the selected strain and construct its initial phylogenetic tree [21]. The assembled sequences were straightened to the NCBI data [22] using the Muscle [23]. In addition, the sequence data were analyzed for phylogenetics based on the NJ method [24] using the program of MEGA version 7 [25]. A thousand resampling for bootstrapping was conducted to determine the validity of each branch.

Secondary metabolites analysis using TLC

A 10 mg/ml extract concentration (10 µl) was placed on a silica TLC plate F_{254} (Merck) and eluted with a mobile phase containing methanol and dichloromethane in a 10:1 ratio. The plate was observed in a UV cabinet at long UV wavelengths (366 nm) and short UV wavelengths (254 nm). After elution, the plate was examined under UV light at 254 and 366 nm. Vanillin sulfate and cerium sulfate were also sprayed onto the eluted TLC plate.

Screening of endophytic fungi from *K. parviflora*: antibacterial and DPPH-antioxidant

Twenty endophytic fungi from *K. parviflora* were identified in the InaCC, BRIN, Cibinong, Bogor. Then, they were preliminary evaluated for their secondary metabolites using TLC, the qualitative antibacterial effect was conducted by disc diffusion, and the quantitative minimum inhibitory concentration (MIC) value was by serial microdilution. The TLC-bioautography method was utilized to screen the activity of antioxidants by DPPH, and colorimetry was employed to ascertain the IC_{50} value.

Antibacterial assay by disc diffusion

Sterile paper discs dripped with 10 µl of extract (10 mg/ml) are placed on MHA media that has been inoculated with bacteria (1×10^5 CFU/ml) toward *S. aureus* and *E. coli*. It was followed by incubation for 24 hours at 37°C for 24 hours. The clear zone around the paper disc is an inhibitory zone for bacterial growth, measuring its diameter.

Antibacterial for determination of MIC value

The active extract was assessed quantitatively for the antibacterial effect through their MIC values through a microdilution technique on 96-well microplates, adhering to the protocol outlined by Praptiwi *et al*. [20] with a range of concentration of 4–256 µg/ml, with chloramphenicol serving as the positive control. The lowest concentration with no color change upon the addition of iodonitrotetrazolium chloride (INT) was the MIC value.

DPPH radical scavenging assay by thin layer chromatography

The antioxidant activity screening method, specifically the analysis of radical DPPH scavenging, was performed using TLC-bioautography with DPPH as the free radical source. A 10 µl of extract aliquot, at 10 mg/ml, was applied to the silica TLC F_{254} plate (Merck, F254). The plate was then sprayed with DPPH in methanol (61.5 µg/ml) and followed by 30 minutes incubation at ambient temperature. Radical scavenger activity was shown by spots or bands with yellowish-white color on the purple plate.

Determining quantitative activity for antioxidants using the DPPH radical free scavenging method (IC_{50} value)

The IC_{50} value for antioxidant activity, *i.e.*, DPPH radical scavenging activity, was conducted on the 96-microwell plate by serial dilution [23]. The IC_{50} value for antioxidant activity—DPPH radical scavenging activity—was determined on a 96-microwell plate through serial dilution.

The concentrations ranged from 4 to 256 µg/ml. The stock solution of extract was 10.24 mg/ml. Methanol p.a (195 µl) was put into a well in A, and 5 µl of extract was added, followed by homogenizing. 100 µl methanol p.a was added to row B (2nd row) and added with 100 µl from the previous well in A and homogenized. The next row used the same procedures, and then a hundred ul was discarded on the last row. After diluting, a hundred µl of 61.5 µg/ml methanolic DPPH solution was put into every well, followed by 90 minutes of incubation in a dark condition. A microplate reader (Varioskan, Thermo Scientific) measured absorbance at 517 nm. Inhibition concentration was calculated following the equation below:

$$IC\ (\%) = (A_{DPPH}\ 100\%\text{-}A_{extract})*100/A_{extract}$$

In which IC: Inhibitory concentration, A: Absorbance

2,2'-Azino-bis-3ethylbenzothiazoline-6-sulfonic acid (ABTS) assay

Potassium persulfate solution (88 µl of 140 mM) was added to ABTS solution (5 ml of 7 mmol/l) and followed by 16 hours of incubation at room temperature in the dark. The mixture was diluted with ethanol p.a. Ethanol was added to attain an initial absorbance of 0.7 at 734 nm. In a 96-well microplate, 290 µl of the diluted ABTS solution was combined with 10 µl of the extract or trolox (as a reference) and allowed to sit at room temperature for 6 minutes in the dark and then read using a spectrophotometer at 734 nm. Trolox at a concentration of 250–1,000 µg/ml was used to construct a curve of calibration. The IC_{50} value was expressed as trolox equivalents (µg/ml).

FRAP assay

The FRAP assay evaluated the extract's capacity to reduce iron from the Fe^{3+}-TPTZ complex (ferric-2,4,6-tripyridyl-s-triazine) to the Fe^{2+}-TPTZ complex [26]. The FRAP reagent was prepared by mixing sodium acetate solution (300 mM), TPTZ solution (10 mM), and Fe[III] solution (20 mM) in a 10:1:1 ratio. Ascorbic acid, at 625–10,000 µg/ml concentrations, was used to create a standard curve. A volume of 20 µl of either the extract or the standard was added to 280 µl of the FRAP reagent in a 96-well microplate. The microplate was then incubated at 37°C for 10 minutes. Absorbance was measured at 593 nm, and the IC_{50} value was expressed as the equivalent of ascorbic acid.

Antidiabetic assay

Activity of alpha-glucosidase inhibitor

A method was performed for measuring the inhibition of α-glucosidase [27]. The sample concentrations were at 5–50 µg/ml, while the α-Glucosidase for starting the reaction was obtained from Wako Pure Chemical Industry. The activity of α-glucosidase was measured based on The amount of p-nitrophenol emitted at 400 nm, which was used to quantify the activity of α-glucosidase. Blanks were used to correct the background absorbance for the extract, replacing the enzyme with 250 µl of phosphate buffer.

The following formula calculated the percentage of inhibition:

$$\%\ inhibition = \frac{(DMSO\ absorbance\text{-}absorbance\ of\ extract)}{(DMSO\ absorbance\text{-}absorbance\ of\ extract)}\ 100$$

The absorbance of the extract is the difference of absorbance value with and without enzymes.

Activity of alpha-amylase inhibitor

The alpha-amylase activity was performed following the protocol α-amylase activity Assay Kit from Sigma-Aldrich MAK009.

Determination of anticancer of MFC-7 and A549

The cancer cell lines of MCF-7 and the A549 were sourced from the American Type Culture Collection and the European Collection of Authenticated Cell Cultures, respectively. MCF-7 cells were maintained in a medium of DMEM, while the cell line of A549 was maintained in an F-12 Ham medium. Both media were supplemented with 10% fetal bovine serum and a 1× antibiotic-antimycotic solution (all reagents from Sigma Aldrich). Approximately 5×10^3 cells per well were cultured into 96-well plates and incubated for 18–24 hours in a 5% CO_2 at 37°C. Post-incubation, the medium was replaced with fresh medium containing test samples at 1.95–500 µg/ml concentration ranges, followed by an additional 48 hours of incubation under the same conditions. Positive and negative controls consisted of 10 µg/ml cisplatin (from TCI Chemicals) and 1% DMSO (from Sigma Aldrich), respectively.

After an additional incubation, the viability of cells was conducted using the 3-[4,5-dimethylthiazol-2-yl]-2,5-diphenyl tetrazolium bromide (MTT) assay. Briefly, 100 µl of culture medium added with 10 µl reagent of MTT (5 mg/ml, Invitrogen) was transferred to each well after the old one was discarded and followed by washing using phosphate-buffered saline (Sigma Aldrich) and 2–3 hours of incubation in the dark. When crystals of formazan were visible, half of the medium was carefully removed, and 100 µl of DMSO was added to each well, followed by thorough mixing using a plate shaker. Absorbance was read at 570 nm by a plate reader (Multiskan GO, Thermo Scientific). Cell viability of the cells (%) was calculated as [{Absorbance of sample—Absorbance of blank} / {Absorbance of negative control—Absorbance of blank} × 100%]. The IC_{50} value was also determined using a line equation. Additionally, cells were observed under an inverted microscope (Olympus CKX53) equipped with a digital camera (Olympus EP50).

Compound identification using LC-HRMS

UHPLC-HRMS analyzed the chemical composition of the selected fungus, such as BwKpRt-1 ethyl acetate extract, according to the method established by Windarsih *et al*. [28]

with a 3 µl injection volume. Mass identification was carried out using Compound Discoverer™ 3.2 software, with peak extraction filtered through the MzCloud database.

Molecular docking studies

Protein data were acquired from the Research Collaboratory for Structural Bioinformatics Protein Data Bank [29]. We selected 4 proteins target as follow: *Homo sapiens* Kelch-like ECH-associated protein 1 (*Hs*KEAP1; PDB ID: 8IXS) inhibitory for antioxidant, *S.aureus* undecaprenyl diphosphate synthase (*Sa*UPPS; PDB ID: 4H8E) inhibitory for antibacterial (inhibit *S. aureus*), *Homo sapiens* epidermal growth factor receptor (*Hs*EGFR; PDB ID: 3W33) inhibitory for anticancer, *Homo sapiens* pancreatic alpha-amilase (HsPAA; PDB ID: 6Z8L) inhibitory for antidiabetic. The preparation of receptors involved the utilization of PyMoL 1.7.4 and MGLTools 1.5.6 [30].

The co-crystallized ligands, water molecules, and cofactors within each receptor were removed, and Gasteiger charges were introduced individually. The two-dimensional chemical structure of the active compound (Equisetin) was initially drawn using ChemDraw Ultra and then converted to its three-dimensional coordinates using the Chem3D Ultra program. The resulting structures that underwent energy minimization through the molecular mechanics and force fields method and were saved in PDB format using the Avogadro 1.91.0. Additionally, non-polar hydrogen atoms within the ligands were combined, and rotatable bonds were defined using MGL Tools 1.5.6 [30].

Molecular docking simulations were conducted using AutoDock Vina 1.1.2 with the default protocol, and the exhaustiveness was set to 12 [30]. For each receptor, a grid box with dimensions of 10–22 points in all directions was established, with a grid spacing of 1 Å centered around the respective co-crystallized ligands. Following the docking computations, the most favorable poses were selected from the top ten models for each target, based on evaluations of their binding energy (ΔG binding, kcal/mol) and non-bond interactions profile. Subsequent analyses of molecular interactions were carried out using LigPlot+ 2.2.8 and PyMoL 1.7.4 software programs. Validation of all docking activities was carried out by redocking the ligand and receptor cocrystal by determining the root mean square deviation (RMSD) value below 2 Å [30].

RESULT AND DISCUSSION

Morphological characters and phylogenetic analysis of *F. equiseti* strain BwKpRt-1

Figure 1 presents the phenotype characteristic of fungal endophyte BwKpRt-1. Characters of the colony on PDA reaching 50–55 mm diameter in a week, fast-growing colonies with a velvety floccose aerial mycelium. Initially, mycelia's color was white; then it became creamish-orange and yellowish-white in reverse after 1 week in the PDA.

Microscopic description—colony morphology on PDA was characterized by hyphae hyaline, unbranched or branched, and septate (monocytic). No sporodochia was detected on the agar medium. Conidiophores emerged from the

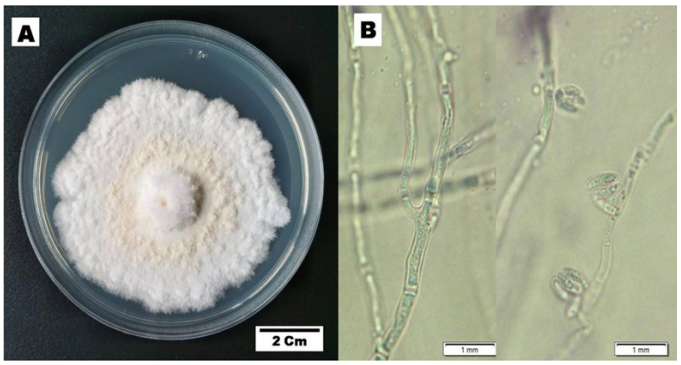

Figure 1. The cultural characteristics of *F. equiseti* strain BwKpRt-1. The culture was grown *in vitro* on PDA media, 10 days incubation at T 27°C.

aerial mycelium, either non-branched, sympodial, or unevenly branched, and have lateral or terminal phialides with poly or monophialidic. The shape could be subcylindrical or subulate, occasionally spreading percurrently, and were smooth, thin-walled, and hyaline. Microconidia: abundant in the aerial mycelia, oval, reniform, elongated oval to sometimes oblong, typically 0-septate, and truncate in base. Macroconidia were extremely sparse and difficult to find, but where present, they were typically three-septate, fusiform with tapered apical cells, and poorly developed. Chlamydospores and sexual morph were not produced.

Host – *K. parviflora* Wall. Ex Baker. geographical distribution – Banyuwangi. The molecular analysis was using the fungal endophyte BwKpRt-1. The partial ITS rDNA sequence of the isolate was then submitted to GenBank, and accession number PP753766 was received. The query length of ITS nucleotides At NCBI (http://www.ncbi.nlm.nlh.gov/), the ITS nucleotides were aligned online and consisted of 543 base pairs.

Table 1. shows the first three closest taxa based on online BLAST alignment. The phylogenetic analysis strengthened this molecular result. Regarding the phylogenetic tree produced from the NJ analysis, the sequence of ITS of fungal endophyte BwKpRt-1 nested in the same clade with *F. equiseti* isolate N-32-1 (MT560375), *F. equiseti* strain CB33-4 (MT558601), and *F. equiseti* strain CB09-3-6 (MT558597) with 88% bootstrap value (Fig. 2). The BLAST result and phylogenetic tree analysis showed that fungal endophyte BwKpRt1 had a similarity of 99.08% to *F. equiseti* (Table 1).

Preliminary analysis for antibacterial and antioxidant of fungal endophytes from *K. parviflora*

Twenty fungal endophytes from *K. parviflora* collected from two places in Indonesia (Bogor and Banyuwangi) were screened for their antibacterial potential against *S. aureus* and *E. coli* (Fig. 3, Table 2), and DPPH-antioxidant properties (Fig. 4, Table 2). The results determined four extracts prevent *S. aureus* growth with MICs of 64–256 µg/ml, and the most potent (MIC: 64 µg/ml) was BwKpRt-1 endophyte.

Screening of DPPH-antioxidant activity by TLC-bioautography indicated several extracts contained DPPH-antioxidant active compounds with a yellowish-white color on

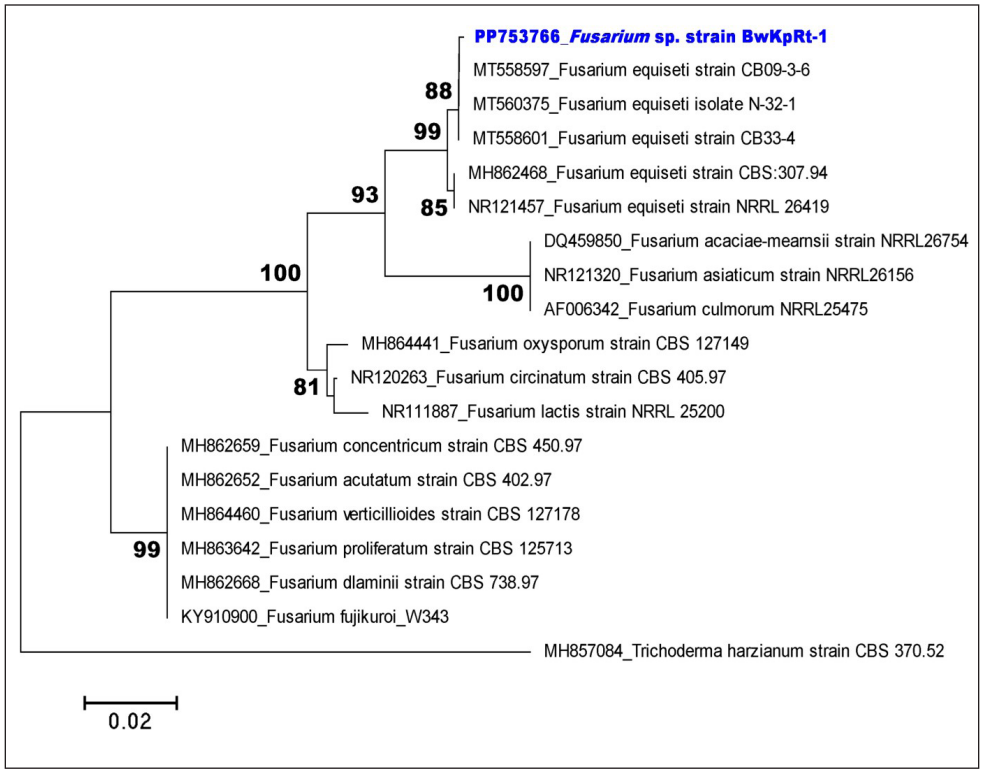

Figure 2. Neighbor-joining tree of selected fungal endophyte *Fusarium* sp. strain BwKpRt-1 based on ITS rDNA sequence and *Trichoderma harzianum* as an outgroup. Only bootstrap values above 80 are shown.

Table 1. The BLAST result of *Fusarium* sp. strain BwKpRt-1 based on ITS rDNA sequence according to NCBI BLAST (https://blast.ncbi.nlm.nih.gov/).

Fungal strain	Genbank acession number	First-third closest taxa on NCBI BLAST (https://blast.ncbi.nlm.nih.gov/)
BwKpRt-1	PP753766	*Fusarium equiseti* isolate N-32-1 (Accession no: MT560375) [Similarity: 99.08%; Max score: 976; Total score: 976; Query coverage: 100%; *E*-value: 0.0; Max identities: 538/543 (99%); Gaps: 0/543(0%)] *Fusarium equiseti* strain CB33-4 (Accession no: MT558601) [Similarity: 99.08%; Max score: 976; Total score: 976; Query coverage: 100%; *E*-value: 0.0; Max identities: 538/543 (99%); Gaps: 0/543(0%)] *Fusarium equiseti* strain CB09-3-6 (Accession no: MT558597) [Similarity: 99.08%; Max score: 976; Total score: 976; Query coverage: 100%; *E*-value: 0.0; Max identities: 538/543 (99%); Gaps: 0/543(0%)]

the TLC plate sprayed with INT (Fig. 4). There were two extracts with moderate DPPH-antioxidant activity, *i.e*., BwKpRt-1 and BwKpRt-2, with an antioxidant activity index (AAI) of 0.5 and 0.4, respectively. Based on the preliminary screening results, the endophytic fungi BwKpRt-1 was the promising endophytic and was further analyzed for its bioactivities.

Antibacterial activity a selected fungal endophyte *F. equiseti* BwKpRT-1

The MIC value determination toward *S. aureus* and *E. coli* by microdilution confirmed that the MIC against *S. aureus* was 64 µg/ml, categorized as a potent antibacterial. However, the value of MIC toward *E. coli* was >256 µg/ml, which is classified as weak antibacterial.

The antibacterial activity test against *Staphylococcus aureus* with a MIC below 100 µg/ml is considered strong for an extract. However, the active compounds must be isolated to compare their efficacy with commercial antibiotics. Methicillin resistance in *S. aureus* (MRSA) is defined by an oxacillin MIC of ≥4 µg/ml [31].

Previous studies have demonstrated that equisetin, a compound derived from marine fungi, exhibits potent antibacterial activity against resistant bacteria such as MRSA and vancomycin-resistant Enterococcus without inducing

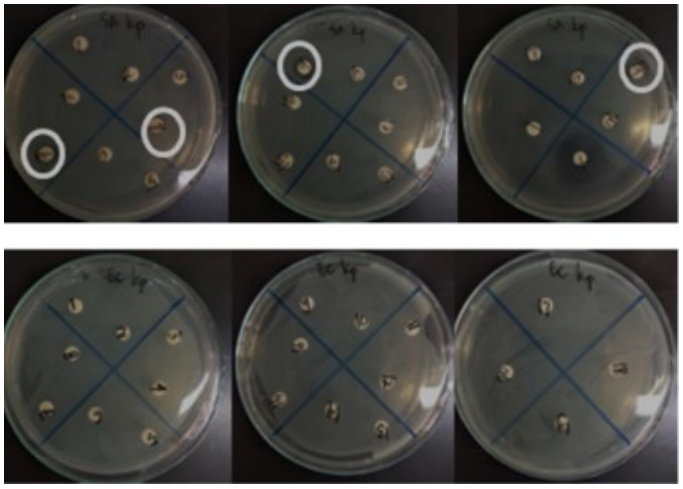

Figure 3. Antibacterial activity of endophytic fungi extracts from *K. parviflora* against *Staphylococcus aureus* (upper) and *Escherichia coli* (lower).

detectable high-level resistance. Additionally, equisetin isolated from the endophytic fungus *Fusarium* sp. JDJR1 has shown both antimicrobial and herbicidal properties [32]. Equisetin also displays strong antibiotic activity against certain Gram-positive bacteria and mycobacteria, further highlighting its potential as an effective antibacterial agent [33].

A previous study by Adione *et al*. [34] showed that fungal endophyte *F. equiseti* isolated from *Ocimum gratissimum* possessed antibacterial against several bacteria. Its antibacterial activity is due to the antibiotic compounds from *F. equiseti,* which are equisetin and epi-equisetin [35]. Marine-derived *F. equiseti* D39 produces six 3-decalinoyltetramic acid derivatives, one of which possesses anti-phytopathogen against *Pseudomonas syringae*, and this compound can be produced in potato liquid culture media with 1% salinity [36]. Based on LC-HRMS results, the extract of *F. equiseti* BwKpRt-1 contains several compounds with bioactivities, such as uracil, sorbic acid, and beauvericin. Beauvericin is a mycotoxin with several

Table 2. Fungal taxa, MIC, IC_{50}, and AAI of endophytic fungi isolated from *K. parviflora.*

No	Code of isolate	Fungal taxa based on morphology	MIC against *S.aureus* (µg/ml)	MIC Against *E.coli* (µg/ml)	IC_{50} (DPPH free radical) (µg/ml)	AAI
1	BgKpB1	*Trichoderma* sp.	>256	>256	>256	–
2	BgKpB2-1	*Trichoderma sp.*	>256	>256	>256	–
3	BgKpB2-2	*Trichoderma* sp.	>256	>256	>256	–
4	BgKpB3-1a	*Trichoderma* sp.	128	>256	>256	–
5	BgKpB4-1a	*Lasiodiplodia* sp.	>256	>256	>256	–
6	BgKpB4-1b	*Lasiodiplodia* sp.	>256	>256	>256	–
7	BgKpB4-2	*Lasiodiplodia* sp.	256	>256	>256	–
8	BgKpB5-1	*Lasiodiplodia* sp.	>256	>256	>256	–
9	BgKpB5-2	*Lasiodiplodia* sp.	256	>256	>256	–
10	BgKpB6-1a	*Trichoderma* sp.	>256	>256	>256	–
11	BgKpB6-2	*Trichoderma* sp.	>256	>256	>256	–
12	BKpB2	*Trichoderma* sp.	>256	>256	>256	–
13	BKpB3-1	*Collelotrichum* sp.	>256	>256	>256	–
14	BKpB3-2	*Collelotrichum* sp.	>256	>256	>256	–
15	DKpB1	*Collelotrichum* cf. *siamense*	>256	>256	>256	–
16	DKpB2	*Collelotrichum* cf. *gloeosporioides*	>256	>256	>256	–
17	DKpB4	*Collelotrichum* cf. *gloeosporioides*	>256	>256	>256	–
18	BwKpB1	Sordariomycetes	>256	>256	>256	–
19	**BwKpRt-1**	***Fusarium* sp.**	**64**	>256	**57.36**	**0.5**
20	BwKpRt-2	*Ceratocystis* sp.	>256	>256	61.54	0.4
	Erythromycin (control)	–	<0.5	16	–	–
	Catechin (control)	–	–	–	7.87	3.9

Notes: m: moderate, MIC: Minimum inhibitory concentration, IC_{50}: Inhibitory Concentration of 50 % DPPH, and AAI: Antioxidant Activity Index (AAI= [Final Concentration of DPPH]/IC_{50}).

Bold letter: active extract with strong antibacterial against *S.aureus* and moderate antioxidant against DPPH.

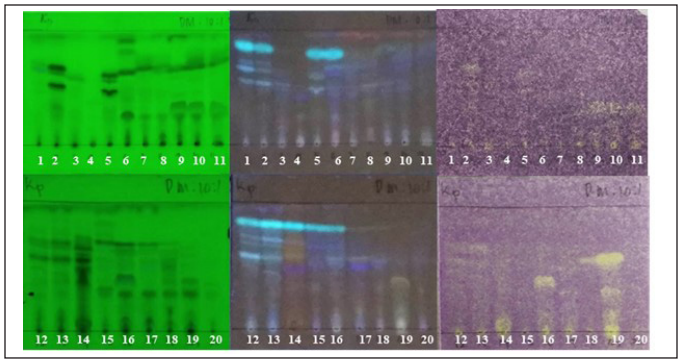

Figure 4. Bioautogram of endophytic fungi from *K. parviflora*, observed under UV 254 nm (left), UV 366 nm (center), sprayed with 0.2% DPPH solution in methanol (right). Upper: observed at 0 minutes after DPPH spraying. Lower: observed at 15 minutes after DPPH spraying. Notes: The active antioxidant compounds are yellowish-white with a purple background.

bioactivities, such as an antibiotic, insecticide, apoptosis inhibitor, ionophore, antifungal agent, P450 inhibitor, and antineoplastic agent [37]. The extract's antibacterial activity toward *S. aureus* was classified as potent antibacterial. The small amount of these compounds might cause it, and they may not work synergistically. Several factors affect secondary metabolite production in endophytic fungi, such as lighting, culture medium composition, pH, agitation, and temperature [38]. Therefore, there is the possibility of variations in activity and the type of secondary metabolite compounds if there are differences in growth media.

Antioxidant assay of a selected fungal endophyte *F. equiseti* BwKpRT-1

Antioxidant activity is useful for assessing the harmful effects of free radicals in living organism systems [39]. The antioxidant properties of the extract of *F. equiseti* BwKpRT-1 were evaluated using several methods, *i.e*., radical scavenger toward DPPH, ABTS, and FRAP (Table 3). The result showed that the IC_{50} value of DPPH radical scavenging activity was 57.36 µg/ml or AAI value 0.5, categorized as moderate antioxidant activity. The evaluation of the antioxidant activity of the BwKpRt-1 extract based on the ABTS method showed that the extract had an IC_{50} of 1.37 mg/ml, while the IC_{50} of the positive control trolox was 0.12 mg/ml. The IC_{50} value of the extract was about 11-fold that of trolox. The higher the IC_{50} value, the lower the antioxidant activity. The higher IC_{50} value means the concentration needed to scavenge half of the radical was significantly higher. Three techniques assessed antioxidant activity based on the capacity to scavenge free radicals.

The result from Table 3 showed that the extract of fungal endophyte BwKpRt1 had an IC_{50} value higher than those of control positive (catechin, trolox, and gallic acid). The antioxidant activity of catechin is based on its scavenging capacity for free radicals through the action of the hydroxyl group [40]. Another positive control used in the antioxidant assay is trolox. A hydrophilic analog of vitamin E, trolox, is a potent radical scavenger with a high capacity to scavenge

Table 3. The IC_{50} of BwKpRT-1 for antioxidant activity using the DPPH, ABTS, and FRAP methods.

Method	Sample	IC_{50} value (µg/ml)
DPPH	BwKpRt1 extract	57.36
	Catechin (control)	7.87
ABTS	BwKpRT1	1.37×10^3
	Trolox (control)	0.12×10^3
FRAP	BwKpRT1	>100
	Gallic acid (control)	0.11×10^3

Table 4. IC_{50} value for α-glucosidase and α-amylase inhibitory activity of the extract of *F. equiseti* BwKpRt1.

Sample	α-amylase activity (nmole/minute/ml)	α-glucosidase activity (unit/l)
Extract of BwKpRt-1	0.121 ± 0.02	335.38
Positive control (nitrophenol)	10.813 ± 0.06	NT
Positive control (quercetin)	NT	3.14

Notes: NT: Not Tested.

peroxyl and alkoxyl radicals [41]. Gallic acid can also scavenge free radicals. The results of the antioxidant analysis showed that BwKpRt1 is considered to have weak antioxidant activity. However, *F. equiseti* ANP2 from mangroves produces exopolysaccharides that could scavenge hydroxyl radicals [42]. The low content of chemical compounds with antioxidant activity might cause low activity as an antioxidant or scavenger of free radicals in the extract of *F. equiseti* BwKpRt-1.

In this research, the antioxidant activity, particularly its moderate ability to scavenge DPPH radicals, was classified as weak in ABTS and FRAP assays. It may be attributed to the antioxidant mechanism of specific components in the extract, such as equisetin, which can donate protons or transfer hydrogen atoms from the hydroxyl group at C-4 on the 5-membered ring. This donating proton (hydrogen) is stabilized by the presence of delocalized electrons from neighboring double bonds at C=O and C=C. This mechanism aligns with previous research suggesting that the DPPH radical (2,2-Diphenyl-1-picrylhydrazyl, DPPH•) scavenging process may involve both single-electron transfer and hydrogen atom transfer reactions [43].

Antidiabetic activity of a selected fungal endophyte *F. equiseti* BwKpRt-1

Antidiabetic activity of *F. equiseti* BwKpRt-1 was performed based on the enzymes of α-amylase and α-glucosidase inhibition (Table 4.). The inhibitory action of α-amylase and α-glucosidase can decrease glucose re-absorption in the intestine (Sim *et al*. 2010).

Based on the result in Table 4, the extract of *F. equiseti* BwKpRt-1 had lower α-amylase and α-glucosidase activity

than positive control of nitrophenol and quercetin. However, the extract of *K. parviflora* reduces the glucose serum level of mice with high-fat diets. The decreased activity of α-glucosidase and α-amylase in *in-vitro* analyses of endophytic fungus extract of *F. equiseti* BwKpRt-1 might be caused by the low level of compounds with antidiabetic activity.

Antiproliferative activity of a selected fungal endophyte *F. equiseti* BwKpRt-1

The fungal endophyte *F. equiseti* BwKpRT-1 extract demonstrated significant antiproliferative activities against cancerous cell lines of MCF-7 (Fig. 5A) and A549 (Fig. 5B). The extract's IC_{50} values were 58.61 µg/ml for MCF-7 cells and 42.64 µg/ml for A549 cells. In addition, *F. equiseti* BwKpRt-1 extracts' ability to inhibit the MCF-7 cell growth was notably seen at 31.25 µg/ml concentration. Interestingly, antiproliferative activity against a cancerous cell of A549 was significantly evident at a concentration under 15.63 µg/ml. It indicates that *F. equiseti* BwKpRt-1 extracts exhibit more potent antiproliferative activity against A549 cells

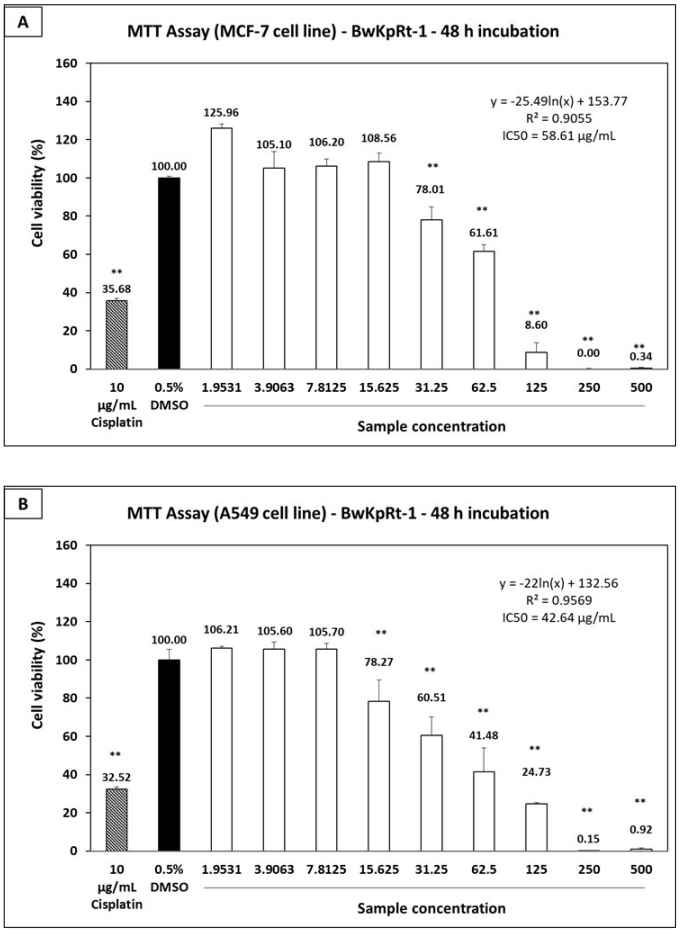

Figure 5. Antiproliferative effect of the fungal endophyte *F. equiseti* BwKpRT-1 extract against (A) breast cancer MCF-7 and (B) lung cancer A549 cell lines. Both cell lines were treated with or without the extract for 48 hours. Statistical analysis was performed using one-way ANOVA followed by the Tukey-Kramer test. Data showing significance against the negative control (0.5% DMSO) is denoted by asterisks $*p < 0.05$; $**p < 0.01$. IC_{50} values were calculated using a line equation.

than MCF-7 cells. The outcomes propose the potential of *F. equiseti* BwKpRt-1 extracts as a promising source of anticancer agents.

Antiproliferative activity against specific cell lines, particularly A549, is likely influenced by the cytotoxic properties of equisetin. Previous studies have reported that equisetin exhibits impressive biological activities, including HIV inhibitory effects, cytotoxicity, DNA binding activity, and mitochondrial ATPase inhibition [44]. Its anticancer activity may involve a DNA binding mechanism, wherein the molecule interacts directly with cancer cell DNA [45]. This interaction disrupts essential processes such as DNA replication, transcription, and repair, thereby impairing the survival and proliferation of cancer cells.

Chemical compounds of a selected fungal endophyte *F. equiseti* BwKpRt-1

Several compounds were present in the extract of *F. equiseti* BwKpRt-1 that were identified using LC-HRMS (Table 5). A possible bioactive compound that plays a role in antimicrobial, antidiabetic, and antioxidant activity from BwKpRt-1 extract is a compound that dominates the extract, known as octahydronaptahalene derivatives, namely (5*R*)-3-[(1*S*,2*R*,4a*S*,6*R*,8a*R*)-1,6-dimethyl-2-[(1*E*)-prop-1-en-1-yl]-1,2,4a,5,6,7,8,8a-octahydronaphthalene-1-carbonyl]-4-hydroxy-5-(hydroxymethyl)-1-methyl-2,5-dihydro-1*H*-pyrrol-2-one) or equisetin with a relative percent composition of about 42.18% (Fig. 6). *Fusarium* sp. PSU-ES 123, isolated from seagrass, also produced octahydronaphtalene derivatives [46].

AMF-26, an octahydronaphthalene derivative, was used to regulate inflammation and angiogenesis in cancerous tumors and other chronic inflammatory conditions [47]. Several octahydronaphthalene derivatives isolated from the endophytic fungus *Trichoderma* sp. also have antifungal activity against *Botrytis cinerea* and *Alternaria alternata* [48], an octahydronaphthalene from the filamentous fungus *Chaetomium* has potential as anti-HIV agent [48]. Besides octahydronaptahalene derivatives, the extract of *F. equiseti* BwKpRT-1 also contains several chemical compounds that may have bioactivities. Uracil may have bioactivities as antitumor, herbicidal, insecticidal, bactericidal, and antiviral [49]. Other compounds with bioactivities are sorbic acid, with antibacterial properties against several bacteria [50]. Beauvericin is a natural product from *F. equiseti* and *F. avenaceum*, with insecticidal, antimicrobial, antiviral, and cytotoxic activities [51].

Molecular docking studies

The validation of all docking activities was conducted through redocking, where the ligand was re-docked into the receptor's binding site to compare its position with the original cocrystal structure. The accuracy of the docking process was assessed by calculating the RMSD value below 2 Å to confirm reliable docking results. In this study, the RMSD values ranged from 0.5 to 1.1 Å (Table 6), indicating a high degree of accuracy and reproducibility in the docking simulations. These values suggest that the docking protocol effectively reproduced

Table 5. Chemical compounds in extract of *F. equiseti* BwKpRt-1 using LC-HRMS.

No	Name	Formula	MW	Positive Ion Mode [M+H]+	RT [minutes]	Area (Max.)	Similarity mzCloud (%)	Relative abundance (%)
1	Uracil	$C_4H_4N_2O_2$	112.03	113.03	0.91	2,784,655,868	98.90	1.78
2	Unknown	C_4H_8O	72.06	73.06	1.16	4,356,852,855	–	2.78
3	Sorbic acid	$C_6H_8O_2$	112.05	113.06	2.80	3,262,936,685	85.70	2.08
4	NP-013736	$C_{10}H_{16}N_2O_2$	196.12	197.13	3.87	3,412,674,421	97.00	2.18
5	N-Acetyltyramine	$C_{10}H_{13}NO_2$	179.09	180.10	4.13	3,542,569,971	99.70	2.26
6	Unknown	$C_{10}H_{13}NO_2$	179.09	180.10	4.60	12,672,200,808	–	8.08
7	NP-011220	$C_{11}H_{18}N_2O_2$	210.14	211.14	5.14	5,945,375,523	95.40	3.79
8	Unknown	$C_{10}H_{13}NO_2$	179.09	180.10	5.19	3,134,407,527	–	2.00
9	NP-011220	$C_{11}H_{18}N_2O_2$	210.14	211.14	5.42	9,083,072,345	94.50	5.79
10	Cyclo(phenylalanyl-prolyl)	$C_{14}H_{16}N_2O_2$	244.12	245.13	6.07	2,898,739,452	97.00	1.85
11	4-Phenylbutyric acid	$C_{10}H_{12}O_2$	164.08	165.09	9.08	5,558,433,412	94.10	3.54
12	Unknown	$C_{15}H_{24}$	204.19	205.19	13.15	3,359,964,437	–	2.14
13	**(5*R*)-3-[(1*S*,2*R*,4a*S*,6*R*,8a*R*)-1,6-dimethyl-2-[(1E)-prop-1-en-1-yl]-1,2,4a,5,6,7,8,8a-octahydronaphthalene-1-carbonyl]-4-hydroxy-5-(hydroxymethyl)-1-methyl-2,5-dihydro-1H-pyrrol-2-one**	$C_{22}H_{31}NO_4$	373.22	374.23	13.58	**66,150,604,696**	97.80	**42.18**
14	1-Linoleoyl glycerol	$C_{21}H_{38}O_4$	354.28	355.28	14.16	2,924,873,459	98.20	1.86
15	9(Z),11(E)-Conjugated linoleic acid	$C_{18}H_{32}O_2$	280.24	279.23*	15.09	5,542,387,051	100.00	3.53
16	Palmitelaidic acid methyl ester	$C_{17}H_{32}O_2$	268.24	269.25	15.25	2,393,724,723	86.00	1.53
17	Unknown	$C_{28}H_{42}O_2$	410.32	411.33	15.38	7,513,335,613	–	4.79
18	Beauvericin	$C_{45}H_{57}N_3O_9$	783.41	784.41	15.65	4,743,064,500	98.70	3.02
19	Unknown	$C_{28}H_{42}O$	394.32	395.33	16.02	7,566,057,794	–	4.82

Notes: (*): Negative ion mode ($[M-H]^-$)

Bold letter: a dominant bioactive compound.

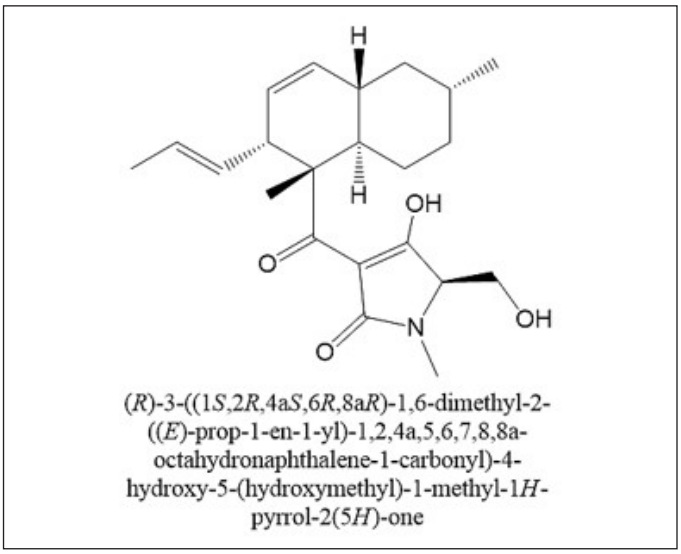

(*R*)-3-((1*S*,2*R*,4a*S*,6*R*,8a*R*)-1,6-dimethyl-2-((*E*)-prop-1-en-1-yl)-1,2,4a,5,6,7,8,8a-octahydronaphthalene-1-carbonyl)-4-hydroxy-5-(hydroxymethyl)-1-methyl-1*H*-pyrrol-2(5*H*)-one

Figure 6. Dominant bioactive compound in the extract of BwKpRt-1.

the experimentally observed binding poses, reinforcing the reliability of the molecular docking analysis.

Our docking results have highlighted that equisetin has better interaction than standard drug at least 2 of the 4 protein targets we examined (Table 6, Fig. 7), *i.e*., as antioxidant (inhibitor *Homo sapiens* Kelch-like ECH-associated protein 1-*Hs*KEAP1; the energy affinities of EQ is lower than standard drug, vitamin C (VitC) with energy affinities are −8.5 and −6.1 Kcal/mol, respectively) and anticancer (inhibitor *Homo sapiens* epidermal growth factor receptor-*Hs*EGFR; the energy affinities of equisetin (EQ) is lower than standard drug, doxorubicin (DXR) with energy affinities are −8.5 and −7.8 Kcal/mol, respectively). *Hs*KEAP1 inhibitors play a crucial role in activating the Nrf2 pathway, which helps protect cells against oxidative stress and inflammation. Meanwhile, *Hs*EGFR is found at abnormally high levels in cancer cells, and *Hs*EGFR activation appears to be important in tumor growth and progression.

The cocrystal ligand of *Hs*KEAP1, identified as T6I (PDB ID: 8IXS), exhibits a complex interaction profile within the binding pocket of the target protein (Table 7). This ligand engages in extensive hydrophobic interactions with multiple amino acid residues, including Ser602, Tyr572, Tyr525, Gly509, Ile461, Gly462, Ala556, Arg415, Ser555, Phe577, Ser508, and Phe478. In addition to these non-polar contacts, T6I establishes hydrogen bonds with Gln530 at a distance of 2.95 Å and Arg483 (3.15 Å), reinforcing its binding affinity and stability within the active site. Similarly, the ligand EQ binds to the same

Table 6. Docking study of cocrystal ligand, standard drug and equisetin against some protein target for antioxidant, antibacterial, anticancer and antidiabetic agents.

No	PDB ID	Protein	Short name	Cocrystal ligand	Standard drug	Function of enzyme	RMSD (Å)	E. affinity Cocrystal ligand (kcal/mol	E. affinity Standard drug (kcal/mol)	E. affinity EQS (kcal/mol)
1	8IXS	*Homo sapiens* Kelch-like ECH-associated protein 1	*Hs*KEAP1	T6I	VitC	KEAP1 inhibitors play a crucial role in activating the Nrf2 pathway, which helps protect cells against oxidative stress and inflammation.	0.617	**−11.8**	-6.1	**−8.5**
2	4H8E	*S.aureus* undecaprenyl diphosphate synthase	*Sa*UPPS	FBB	STR	Bacterial undecaprenyl diphosphate synthase, an essential enzyme involved in cell wall biosynthesis.	1.118	−12.1	−7.5	−6.2
3	3W33	*Homo sapiens* Epidermal growth factor receptor	*Hs*EGFR	W19	DXR	EGFR is found at abnormally high levels in cancer cells, and EGFR activation appears to be important in tumor growth and progression.	0.771	**−13.5**	−7.8	**−8.5**
4	6Z8L	*Homo sapiens* pancreatic alpha-amilase	*Hs*PAA	GLC	ACR	Human pancreatic alpha-amylase is an enzyme that plays a crucial role in breaking down carbohydrates into simpler sugars. Inhibiting this enzyme can help manage blood glucose levels, making it a potential target for treating type 2 diabetes.	0.509	−7.6	−8.3	−7.5

Notes: RMSD: Root Mean Square Deviation of redocking cocrystal ligand. **Standard drug** (VitC: Vitamin C, STR: Streptomycin, DXR: Doxorubicin, ACR: Acarbose). **Cocrystal ligand** (T6I: (2R,3S)-3-[[(2S)-2-fluoranyl-2-(5,6,7,8-tetrahydronaphthalen-2-yl)ethanoyl]amino]-2-methyl-3-(4-methylphenyl)propanoic acid, FBB: farnesyl diphosphate, W19: 4-{[4-(1-benzothiophen-4-yloxy)-3-chlorophenyl]amino}-N-(2-hydroxyethyl)-8,9-dihydro-7H-pyrimido[4,5-b]azepine-6-carboxamide, GLC: alpha-D-glucopyranose-(1-4)-alpha-D-glucopyranose).**EQS**: Equisetin.

Bold numbers on energy affinity: Equisetin's energy affinity is better than the standard drug.

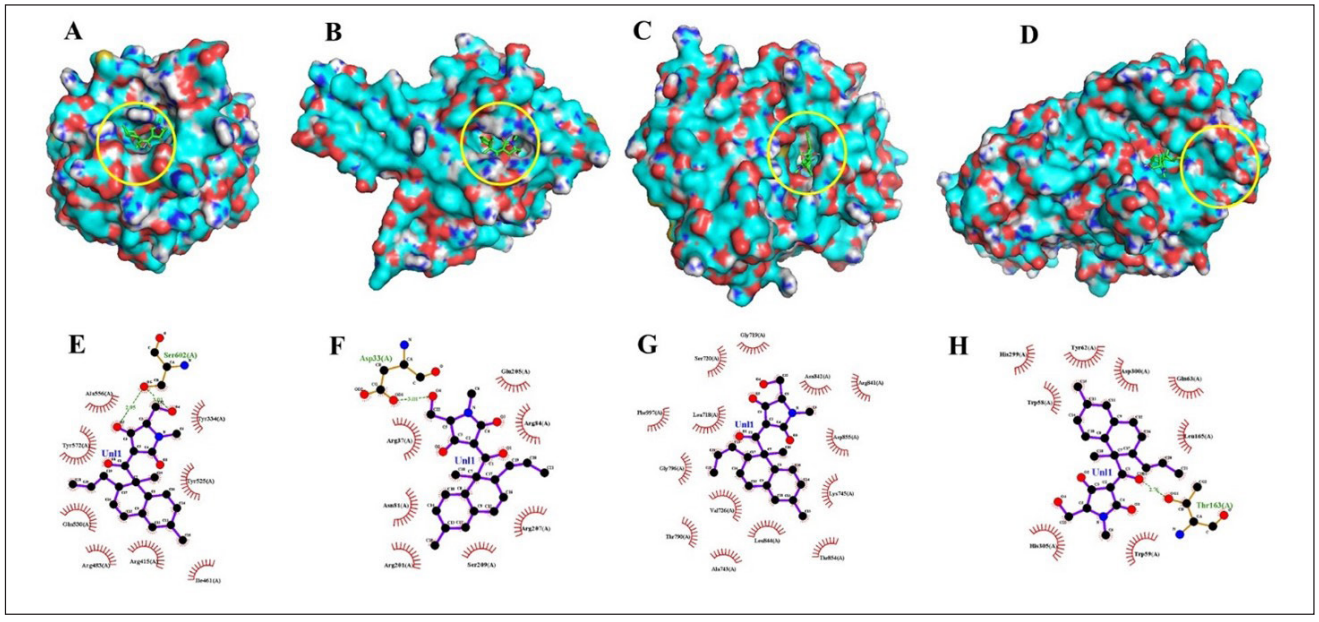

Figure 7. Docking study (3 dan 2 dimension interaction) of equisetin against some protein target for antioxidant (A, E), antibacterial (B, F), anticancer (C, G) and antidiabetic agents (D, H).

Yellow circle: Active site of the protein where the ligand EQ interacts.

Table 7. Interaction of cocrystal ligand, standard drug and equisetin against selected two protein targets.

No	PDB ID	Name Protein	Cocrystal ligand	Standard drug	Interaction with protein					
					Cocrystal ligand		Standard drug		Equisetin	
					Hydrophobic interaction	Hydrogen binding	Hydrophobic interaction	Hydrogen binding	Hydrophobic interaction	Hydrogen binding
1	8IXS	*Hs*KEAP1	T6I	VitC	Ser602; Tyr572; Tyr525; Gly509; Ile461; Gly462; Ala556; Arg415; Ser555; Phe577; Ser508; Phe478	Gln530 (2.95); Arg483 (3.15)	Gln364; Gly603; Gly509; Gly462; Ala556; Arg415	Val604 (3.24); Leu365 (2.82); Leu557 (2.99; 3.05); Ala510 (3.10; 3.11); Val463 (3.31)	Tyr572; Gln530; Tyr525; Arg483; Ile461; Ala556; Arg415; Tyr334	Ser602 (2.95; 3.01)
2	3W33	*Hs*EFGR	W19	DXR	Lys745; Leu858; Thr854; Phe856; Asp855; Leu788; Gly719; Leu718; Leu792; Gly791; Leu844; Ala743; Val726; Thr790; Cys775; Arg776; Leu777	Ser720 (3.03); Met793(3.01; 3.04)	Thr854; Leu858; Asp855; Leu788; Gly719; Asn842; Gly721; Ser720; Leu718; Leu844; Arg841; Val726; Cys775; Leu777	Lys745 (3.25); Met793(3.12); Thr790 (2.77)	Lys745; Thr854; Asp855; Asn842; Arg841; Gly719; Ser720; Leu718; Gly796; Phe997; Leu844; Ala743; Val790	–

Notes: *Hs*KEAP1: Homo sapiens Kelch-like ECH-associated protein 1; *Hs*EFGR: Homo sapiens Epidermal growth factor receptor. **Standard drug** (VitC: Vitamin C, DXR: Doxorubicin). **Cocrystal ligand** (T6I: (2R,3S)-3-[[(2S)-2-fluoranyl-2-(5,6,7,8-tetrahydronaphthalen-2-yl)ethanoyl]amino]-2-methyl-3-(4-methylphenyl) propanoic acid, W19: 4-{[4-(1-benzothiophen-4-yloxy)-3-chlorophenyl]amino}-N-(2-hydroxyethyl)-8,9-dihydro-7H-pyrimido[4,5-b]azepine-6-carboxamide.

binding pocket, forming a hydrogen bond with Ser602 (2.90 Å). Additionally, EQ interacts through hydrophobic contacts with several key residues, including Tyr572, Gln530, Tyr525, Arg483, Ile461, Ala556, Arg415, and Tyr334 (Fig. 7). Notably, despite their structural differences, both T6I and EQ exhibit a considerable degree of overlap in their interaction patterns, sharing common binding site interactions with Ser602, Tyr572, Gln530, Tyr525, Arg483, Ile461, Ala556, and Arg415. While vitamin C (VitC) interact through hydrophobic contacts (with several key residues: Gln364, Gly603, Gly509. Gly462, Ala556 and Arg415) and hydrogen bonds with some residues: Val604 (3.24), Leu365 (2.82), Leu557 (2.99; 3.05), Ala510 (3.10; 3.11), and Val463 (3.31). In other study, interaction between esculetin and KEAP1, it was established that esculetin tightly binds KEAP1 forming hydrogen bonds (Arg483 and Ala556) and hydrophobic interaction (Ser508, Ser555, Gln530, Gly462 and Ile461) [52].

The epidermal growth factor receptor (EGFR) plays a significant role in cell growth and survival, but its overexpression is often associated with cancer progression. The interaction analysis of EGFR (PDB ID: 3W33) with three ligands—EQ, cocrystal ligand (W19), and doxorubicin (DXR, standard drug)—reveals critical binding residues that contribute to ligand affinity and stability. The EQ ligand primarily interacts with Lys745, Thr854, Asp855, and Asn842, forming key hydrogen bonds and electrostatic interactions (Table7, Fig. 7). Meanwhile, W19 exhibits a more extensive binding profile, engaging residues like Leu858, Phe856, Leu788, and Met793 (3.01 Å, 3.04 Å), which contribute to its stability through both hydrogen bonding and hydrophobic interactions. Similarly, DXR forms strong interactions with EGFR, notably involving Lys745 (3.25 Å), Thr790 (2.77 Å), Met793 (3.12 Å), and Arg841, which enhance its binding affinity. The frequent occurrence of residues such as Lys745, Asp855, and Thr790 across multiple ligand interactions suggests that they are critical for EGFR binding and may serve as important targets for drug development. In another study, protein of EGFR interaction with Osimertinib revealed amino acids at the binding pocket of the receptors that includes hydrophobic bonding (with residues including Leu 718, Val726, Ala743, Lys745, Met790, Gln791, Leu792, Pro794, Asp800, Leu844, and Leu1001), and hydrogen bond interaction with Ser797 [53].

CONCLUSION

The study on the identification of fungal endophytes from *K. parviflora* rhizome, identification of compounds, and bioactivities evaluation of the extract of this endophytic fungus showed that the endophytic fungus BwKpRt-1 was identified as *F. equiseti.* The main compound of the extract was equisetin (42.18 %), with several minor compounds that have been known to have bioactivity, such as uracil, sorbic acid, and beauvericin. The extract of *F. equiseti* BwKpRt-1 has the potential to be strong antibacterial against Gram-positive *S. aureus* Ina-CC B2 (<100 µg/ml), moderate antioxidant as DPPH radical free scavenging (IC_{50} value of 57.36 µg/ml or AAI value of 0.5), good antidiabetic activity as inhibitory α-amylase (IC_{50} value of 0.121 ± 0.02 nmole/minute/ml), and good anticancer against MCF-7 and A549 cell lines (IC_{50} value < 100 µg/ml). Docking study revealed that the dominant compounds (equisetin; EQ) exhibits stronger antioxidant and anticancer potential than standard drugs. These findings highlight the potential of *F. equiseti* BwKpRt-1 as a promising source of bioactive compounds for drug development. Further research focusing on isolating and characterizing bioactive compounds, optimizing extraction methods, and *in vivo* studies will be essential to validate and harness these bioactivities for pharmaceutical applications.

ACKNOWLEDGMENT

The authors thank you for supporting the scientific facilities and technically through ELSA-BRIN, especially the Advanced Characterization Laboratories Yogyakarta. The authors are also grateful to Uvi K., Lina Marlina, Andi Saptaji Kamal, and Lukman Hafid for their assistance in laboratory work.

AUTHOR CONTRIBUTIONS

All authors made substantial contributions to conception and design, acquisition of data, or analysis and interpretation of data; took part in drafting the article or revising it critically for important intellectual content; agreed to submit to the current journal; gave final approval of the version to be published; and agree to be accountable for all aspects of the work. All the authors are eligible to be an author as per the International Committee of Medical Journal Editors (ICMJE) requirements/guidelines.

FINANCIAL SUPPORT

National Research and Innovation Agency, Indonesia.

CONFLICTS OF INTEREST

The authors report no financial or any other conflicts of interest in this work.

ETHICAL APPROVALS

This study does not involve experiments on animals or human subjects.

DATA AVAILABILITY

All data generated and analyzed are included in this research article.

PUBLISHER'S NOTE

This journal remains neutral with regard to jurisdictional claims in published institutional affiliation.

REFERENCES

1. Socfindoconservation.co.id [Internet]. *Kaempferia parviflora*. [Cited 2024 Sep 5]. Available from https://www.socfindoconservation.co.id/plant/535?lang=en
2. Powo.science.kew.org [Internet]. *Kaempferia parviflora.* [Cited 2024 Sep 5]. Available from https://powo.science.kew.org/taxon/urn:lsid:ipni.org:names:797188-1
3. Yee TT, Lwin KWY. Study of phytochemical composition on *Kaempferia parviflora* Wall. Ex Baker . IEEE-SEM. 2019;7(7):128–36.
4. Wattanathorn J, Muchimapura S, Tong-Un T, Saenghong N, Thukhum-Mee W, Sripanidkulchai B. Positive modulation effect of 8-week consumption of *Kaempferia parviflora* on health-related physical fitness and oxidative status in healthy elderly volunteers. Evid Based Complement Alternat Med. 2012;2012:732816.
5. Sae-Wong C, Matsuda H, Tewtrakul S, Tansakul P, Nakamura S, Nomura Y, *et al.* Suppressive effects of methoxyflavonoids isolated from *Kaempferia parviflora* on inducible nitric oxide synthase (iNOS) expression in RAW 264.7 cells. J Ethnopharmacol. 2011;136(3):488–95.
6. Tewtrakul S, Subhadhirasakul S, Kummee S. Anti-allergic activity of compounds from *Kaempferia parviflora*. J Ethnopharmacol. 2008;116(1):191–3.
7. Leardkamolkarn V, Tiamyuyen S, Sripanidkulchai B. Pharmacological activity of *Kaempferia parviflora* extract against human bile duct cancer cell lines. Asian Pac J Cancer Prev. 2009;10(4):695–8.
8. Akase T, Shimada T, Terabayashi S, Ikeya Y, Sanada H, Aburada M. Antiobesity effects of *Kaempferia parviflora* in spontaneously obese type II diabetic mice. J Nat Med. 2011;65(1):73–80.
9. Azuma T, Kayano S, Matsumura Y, Konishi Y, Tanaka Y, Kikuzaki H. Antimutagenic and α-glucosidase inhibitory effects of constituents from *Kaempferia parviflora*. Food Chem. 2011;125(2):471–5.
10. Jeong D, Kim DH, Chon JW, Kim H, Lee SK, Kim HS, *et al.* Antibacterial effect of crude extracts of *Kaempferia parviflora* (Krachaidam) against cronobacter spp. and Enterohemorrhagic *Escherichia coli* (EHEC) in various dairy foods: a preliminary study. J Milk Sci Biotechnol. 2016;34(2):63–8.
11. Labrooy CD, Abdullah TL, Abdullah NAP, Stanslas J. Optimum shade enhances growth and 5,7-Dimethoxyflavone accumulation in *Kaempferia parviflora* Wall. ex Baker cultivars. Sci Hortic (Amsterdam). 2016;213:346–53.
12. Sharma P, Singh SP. Chapter 11—Role of the endogenous fungal metabolites in the plant growth improvement and stress tolerance. In: Sharma VK, Shah MP, Parmar S, Kumar A, editors. Fungi Bio-Prospects Sustain. Agric. Environ. Nano-technology. London, UK: Academic Press; 2021. pp 381–401.
13. Anand U, Pal T, Yadav N, Singh VK, Tripathi V, Choudhary KK, *et al.* Current scenario and future prospects of endophytic microbes: promising candidates for abiotic and biotic stress management for agricultural and environmental sustainability. Microb Ecol. 2023;86(3):1455–86.
14. Yang SX, Zhao WT, Chen HY, Zhang L, Liu TK, Chen HP, *et al.* Aureonitols A and B, Two New C(13) -polyketides from *Chaetomium globosum*, an endophytic fungus in *Salvia miltiorrhiza*. Chem Biodivers. 2019;16(9):e1900364.
15. Ujam NT, Adonu CC, Gugu TH, Onwusoba RC, Ike CJ, Offiah RO, *et al.* Assessment of antiplasmodial and immunomodulatory activities of endophytic fungal metabolites from Azadirachta Indica A. Juss. Afr J Microbiol Res. 2022;6(3):121–31.
16. Alisaac E, Mahlein AK. Fusarium head blight on wheat: biology, modern detection and diagnosis and integrated disease management. Toxins (Basel). 2023;15(3):192.
17. Hami A, Rasool RS, Khan NA, Mansoor S, Mir MA, Ahmed N, *et al.* Morpho-molecular identification and first report of *Fusarium equiseti* in causing chilli wilt from Kashmir (Northern Himalayas). Sci Rep. 2021;11(1):3610.
18. Liu S, Gao W, Yang X, Huo R, Chen F, Cao F, *et al.* Structure determination and cytotoxic evaluation of metabolites from the entomogenous fungus *Fusarium equiseti*. J Antibiot (Tokyo). 2021;74(3):176–80.
19. Pham GN, Josselin B, Cousseau A, Baratte B, Dayras M, Le Meur C, *et al.* New fusarochromanone derivatives from the marine fungus *Fusarium equiseti* UBOCC-A-117302. Mar Drugs. 2024;22(10):444.
20. Praptiwi, Fathoni A, Ilyas M. Diversity of endophytic fungi from *Vernonia amygdalina*, their phenolic and flavonoid contents and bioactivities. Biodiversitas. 2020;21(2):436–41.
21. Technelysium.com.au [Internet]. *Chromaspro*. [Cited 2024 Aug 1]. Available from http://technelysium.com.au/wp/chromaspro/
22. Ncbi.nlm.nih.gov [Internet]. *NCBI*. [Cited 2024 Aug 1]. Available from https://www.ncbi.nlm.nih.gov/
23. Ebi.ac.uk [Internet]. *Muscle*. [Cited 2024 Aug 1]. Available from http://www.ebi.ac.uk/Tools/msa/muscle
24. Saitou N, Nei M. The neighbor-joining method: a new method for reconstructing phylogenetic trees. Mol Biol Evol. 1987;4:406–25.
25. Kumar S, Stecher G, Tamura K. MEGA7: Molecular evolutionary genetics analysis version 7.0 for bigger datasets. Mol Biol Evol. 2016;33:1870–4.

26. Amarowicz R, Pegg RB. Chapter one—natural antioxidants of plant origin. In: Ferreira ICFR, Barros LBT-A in F and NR, editors. Funct. Food Ingredients from Plants. Academic Press; 2019. Vol. 90, 1–81.
27. Kim KY, Nam KA, Kurihara H, Kim SM. Potent alpha-glucosidase inhibitors purified from the red alga Grateloupia elliptica. Phytochemistry. 2008;69(16):2820–5.
28. Windarsih A, Suratno, Warmiko HD, Indrianingsih AW, Rohman A, Ulumuddin YI. Untargeted metabolomics and proteomics approach using liquid chromatography-Orbitrap high resolution mass spectrometry to detect pork adulteration in *Pangasius hypopthalmus* meat. Food Chem. 2022;386:132856.
29. Rcsb.org [Internet]. RCSB Protein Data Bank. [Cited 2025 Feb 3]. Available from https://www.rcsb.org/.
30. Nurkanto A, Masrukhin, Erdian Tampubolon JC, Ewaldo MF, Putri AL, Ratnakomala S, *et al.* Exploring Indonesian actinomycete extracts for anti-tubercular compounds: integrating inhibition assessment, genomic analysis, and prediction of its target by molecular docking. Heliyon. 2024;10(15):e35648.
31. Rybak MJ, Akins RL. Emergence of methicillin-resistant *Staphylococcus aureus* with intermediate glycopeptide resistance. Drugs. 2001;61(1):1–7.
32. Wei W, Chen P, Khan B, Tian K, Feng Y, Lv B, *et al.* Evaluation of Equisetin as an anti-microbial and herbicidal agent from endophytic fungus Fusarium sp. JDJR1. Agronomy. 2024;14(1):31
33. Chen S, Liu D, Qi Z, Guo P, Ding S, Shen J, *et al.* A marine antibiotic kills multidrug-resistant bacteria without detectable high-level resistance. ACS Infect Dis. 2021;7:884–93.
34. Adione NM, Onyeka IP, Abba CC, Okoye NN, Eze PM, Umeokoli BO, *et al.* Antimicrobial activities of the endophytic fungus, *Fusarium equiseti*, isolated from the leaves of *Ocimum gratissimum*. J Adv Med Pharm Sci. 2022;24(7):11–23.
35. Burmeister HR, Bennett GA, Vesonder RF, Hesseltine CW. Antibiotic produced by *Fusarium equiseti* NRRL 5537. Antimicrob Agents Chemother. 1974;5(6):634–9.
36. Zhao D, Han X, Wang D, Liu M, Gou J, Peng Y, *et al.* Bioactive 3-decalinoyltetramic acids derivatives from a marine-derived strain of the fungus *Fusarium equiseti* D39. Front Microbiol. 2019;10:1285.
37. Pubchem.ncbi.nlm.nih.gov [Internet]. Beauvericin. [Cited 2024 Sep 5]. Available from https://pubchem.ncbi.nlm.nih.gov/compound/3007984
38. Venugopalan A, Srivastava S. Endophytes as *in vitro* production platforms of high value plant secondary metabolites. Biotechnol Adv. 2015;33(6 Pt 1):873–87.
39. Lahmass I, Ouahhoud S, Elmansuri M, Sabouni A, Elyoubi M, Benabbas R, *et al.* Determination of antioxidant properties of six by-products of *Crocus sativus* L. (Saffron) plant products. Waste Biomass Valorization. 2018;9(8):1349–57.
40. Munteanu IG, Apetrei C. Assessment of the antioxidant activity of catechin in nutraceuticals: comparison between a newly developed electrochemical method and spectrophotometric methods. Int J Mol Sci. 2022;23(15):8110.
41. Giordano ME, Caricato R, Lionetto MG. Concentration dependence of the antioxidant and prooxidant activity of trolox in heLa cells: involvement in the induction of apoptotic volume decrease. Antioxidants (Basel, Switzerland). 2020;9(11):1058.
42. Prathyusha AMVN, Mohana Sheela G, Bramhachari PV. Chemical characterization and antioxidant properties of exopolysaccharides from mangrove filamentous fungi *Fusarium equiseti* ANP2. Biotechnol Reports. 2018;19:e00277.
43. Sadowska-Bartosz I, Bartosz G. Antioxidant activity of anthocyanins and anthocyanidins: a critical review. Int J Mol Sci. 2024;25(22):12001.
44. Eze PM, Abonyi DO, Abba CC, Proksch P, Okoye FBC, Esimone CO. Toxic, but beneficial compounds from endophytic fungi of Carica papaya. EuroBiotech J. 2019;3(2):105–11.
45. Alotaibi SH, Momen AA. Anticancer drugs' deoxyribonucleic acid (DNA) interactions. In: Khalid MAA, editor. Biophysical chemistry—advance applications. Rijeka, Croatia: IntechOpen; 2019.
46. Saetang P, Rukachaisirikul V, Phongpaichit S, Sakayaroj J, Shi X, Chen J, *et al.* β-Resorcylic macrolide and octahydronaphthalene derivatives from a seagrass-derived fungus *Fusarium* sp. PSU-ES123. Tetrahedron. 2016;72(41):6421–7.
47. Watari K, Nakamura M, Fukunaga Y, Furuno A, Shibata T, Kawahara A, *et al.* The antitumor effect of a novel angiogenesis inhibitor (an octahydronaphthalene derivative) targeting both VEGF receptor and NF-κB pathway. Int J Cancer. 2012;131(2):310–21.
48. Wu JL, Yu YH, Yao HZ, Zhao X, Yuan T, Huang YH. Trichodermic acids from an endophytic Trichoderma sp. and their antifungal activity against the phytopathogen Botrytis cinerea. Phytochem Lett. 2023;56:24–9.
49. Pałasz A, Cież D. In search of uracil derivatives as bioactive agents. Uracils and fused uracils: synthesis, biological activity and applications. Eur J Med Chem. 2015;97:582–611.
50. Wei Q, Wang X, Cheng JH, Zeng G, Sun DW. Synthesis and antimicrobial activities of novel sorbic and benzoic acid amide derivatives. Food Chem. 2018;268:220–32.
51. Wang Q, Xu L. Beauvericin, a bioactive compound produced by fungi: a short review. Molecules. 2012;17(3):2367–77.
52. Adelusi TI, Abdul-Hammed M, Idris MO, Oyedele QK, Adedotun IO. Molecular dynamics, quantum mechanics and docking studies of some Keap1 inhibitors—an insight into the atomistic mechanisms of their antioxidant potential. Heliyon. 2021;7(6):e07317.
53. Kashima K, Kawauchi H, Tanimura H, Tachibana Y, Chiba T, Torizawa T, *et al.* CH7233163 Overcomes Osimertinib-resistant EGFR-Del19/T790M/C797S Mutation. Mol Cancer Ther. 2020;19(11):2288–97.

How to cite this article:
Praptiwi P, Ilyas M, Putra ABN, Palupi KD, Fathoni A, Lotulung PDN, Evana E, Rahmi D, Agusta A. Bioactivity evaluation of compounds produced by *Fusarium equiseti* from *Kaempferia parviflora* rhizome from Indonesia. J Appl Pharm Sci. 2025;15(07):179–192. DOI: 10.7324/JAPS.2025.221818